

Thermally Driven Circulations in Small Oceanic Basins

Joseph Pedlosky
Woods Hole Oceanographic Institution
Woods Hole, MA 02543

December 16, 2002

Woods Hole Oceanographic Contribution number: #####

e-mail: jpedlosky@whoi.edu

Abstract

A linear, steady model of the circulation of a small (f-plane) oceanic basin, driven by heating or cooling at the surface is considered in order to examine the partition of upwelling (heating) or downwelling (cooling) between the basin's interior and its boundary layers on the side wall in which frictional dissipation and lateral temperature diffusion are dominant. The basin is rectangular in plan form. On three of its lateral sides the basin is insulated to heat exchange while on the fourth side the heat added at the surface is shown to be removed through a thin sublayer which also closes the mass balance. The temperature is linearized about a basic linear stratification.

The analytical solution shows that in the case of heating (cooling) in the basin interior, most of the resulting upwelling (downwelling) near the upper surface actually occurs in narrow boundary layers whose width is of the order of the deformation radius rather than in the interior directly. This rather non-intuitive result is consistent with numerical calculations recently performed by Spall (2002) and suggests the distribution of vertical motion between interior and boundary layers is a robust one not dependent on particular parameterizations of eddy fluxes of heat.

1. Introduction

In a recent paper Spall (2002) numerically modeled the circulation in a small (f-plane) oceanic basin connected to a passive, large, open ocean through a narrow passageway . The small basin is cooled and develops a strong eddy field which transports buoyancy to the vicinity of the lateral boundaries of the basin. Sinking motion is found to take place preferentially in the vicinity of the boundary in spite of the concentration of the cooling in the interior of the basin. The heat balance of the basin as a whole is provided for by heat and mass exchange through a narrow seaway connecting the small, marginal sea to a passive open ocean. The actual mass exchange is slight compared to the resulting eddy-induced circulation within the basin but is vital in the model for achieving the heat exchange through the seaway in order to balance the cooling at the surface.

The principal, non-intuitive result obtained by Spall is that the major vertical mass flux in response to the surface cooling is manifested in a narrow zone near the basin boundaries and not in the region directly cooled in the basin interior. Spall argues that this is the result of the need of the fluid to expunge the relative vorticity produced by the stretching due to the vertical motion and that this can be done only in regions of enhanced lateral diffusion of vorticity, i.e. near the boundary. This argument seems so general that it is likely to be more robust than the particular model. Indeed, Spall rationalizes his results with the aid of simple, quasi linear models of the boundary layer process.

In this paper I investigate this process further by examining ab initio a highly idealized, linearized model in which a stably stratified fluid is heated or cooled at the surface and is allowed heat exchange through only a segment of its lateral boundary. The basin is rectangular and three of its lateral boundaries are insulated to heat exchange while the fourth is held at a fixed temperature. No mass exchange through the basin walls is considered as a test of the necessity of such mass exchange to produce the results already described. The analytical theory is focused on the question of the partition between the

vertical motion produced in interior of the basin and the vertical motion in side wall boundary layers whose scale is of the order of the deformation radius. Since the basin is closed to mass exchange the vertical mass balance requires an additional thinner boundary layer on the single non insulating wall of the basin. The compensating mass flux in that thin layer also serves to balance the basin's heat flux with the exterior of the basin in analogy with the mass exchange in Spall's model.

An even simpler model, suitable for laboratory experimentation is also briefly described in which the basin is circular, the motion axisymmetric and the compensating mass flux occurs symmetrically around the basin. The interior to boundary layer partition of the vertical mass flux is the same as in the former case.

2. Theory

The model used here is the linear model of Barcilon and Pedlosky (1967) as altered by Pedlosky (1974) to include distinct mixing coefficients for vertical and horizontal mixing of mass and momentum. (See also Pedlosky et. al. (1997) for a comparison of the theory with experiment in a somewhat different context). Many of the results of those earlier studies are quoted herein rather than rederived.

The fluid is stably stratified with a constant buoyancy frequency and is contained in a rectangular basin as shown in Figure 1. The fluid is contained within rigid boundaries. Scales L_{scale} and D are used to scale the horizontal and vertical independent variables, respectively. In terms of those scales the dimensions of the basin are L in the x direction, l in the y direction and d in the vertical direction. On the basin's lateral boundaries the fluid is insulated to heat exchange. On the fourth side of the basin the temperature is fixed at the temperature established by the basic state temperature whose linear vertical variation provides the basic stratification. On the upper surface the fluid is heated or cooled by a small amount such that within the fluid the temperature variation from the imposed stable vertical stratification is small. Thus the temperature in the fluid is given by:

$$T_{total} = \Delta T_v * (z/d) + \Delta T_h * T(x,y,z), \quad (2.1 \text{ a,b})$$

$$\Delta T_h \ll \Delta T_v.$$

where ΔT_h is the scale of the variable temperature within the fluid which drives the motion.

On the upper surface the fluid is heated by an amount $H*h(x,y)$ where H is the scale of the imposed heating. The scale ΔT_h is chosen such that

$$\Delta T_h = HD/\kappa_v \quad (2.2)$$

where κ_v is the coefficient of vertical diffusivity. In terms of these scales the thermal boundary conditions are:

$$\frac{\partial T}{\partial y} = 0, \quad y = 0, l.$$

$$\frac{\partial T}{\partial x} = 0, \quad x = 0,$$

$$T = 0, \quad x = L,$$

$$\frac{\partial T}{\partial z} = h(x,y), \quad z = d.$$

(2.3 a,b,c,d)

while

$$\frac{\partial T}{\partial z} = 0, \quad z = 0. \quad (2.3 \text{ e})$$

where $h(x,y)$ is the form of the applied heating on the upper surface.

The horizontal velocity scale is $U = \frac{g\alpha\Delta T_h D}{f L_{scale}}$ where α is the coefficient of thermal

expansion and f is the constant Coriolis parameter. A linear equation of state relating

temperature and density is assumed. The vertical velocity scale is UD/L_{scale} and the pressure variation its value in the resting state is scaled hydrostatically. This leads to the following linearized equations for the model:

$$u = -\frac{\partial p}{\partial y} + \frac{E_v}{2} \frac{\partial^2 v}{\partial z^2} + \frac{E_h}{2} \nabla_h^2 v,$$

$$v = \frac{\partial p}{\partial x} + \frac{E_v}{2} \frac{\partial^2 u}{\partial z^2} + \frac{E_h}{2} \nabla_h^2 u,$$

$$0 = -\frac{\partial p}{\partial z} + T + \frac{D^2}{L_{scale}^2} \left[\frac{E_v}{2} \frac{\partial^2 w}{\partial z^2} + \frac{E_h}{2} \nabla_h^2 w \right], \quad (2.4 \text{ a,b,c,d,e})$$

$$\frac{\partial u}{\partial x} + \frac{\partial v}{\partial y} + \frac{\partial w}{\partial z} = 0,$$

$$wS = \frac{E_v}{2\sigma_v} \frac{\partial^2 T}{\partial z^2} + \frac{E_h}{2\sigma_h} \nabla_h^2 T.$$

and

$$\nabla_h^2 = \frac{\partial^2}{\partial x^2} + \frac{\partial^2}{\partial y^2}$$

The parameters appearing in the above non-dimensional equations are the Ekman numbers and Prandtl numbers, i.e.:

$$\begin{aligned} E_h &= 2\nu_h / f L_{scale}^2, & E_v &= 2\nu_v / f D^2, \\ \sigma_h &= \nu_h / \kappa_h, & \sigma_v &= \nu_v / \kappa_v \end{aligned} \quad (2.5 \text{ a,b,c,d})$$

where the coefficients of momentum mixing ν_v, ν_h are taken to be possibly different in the horizontal and vertical directions, and similarly with the heat diffusion coefficients. For a

laboratory model one would take them to be equal. The stratification parameter S is defined as:

$$S = \frac{N^2 D^2}{f^2 L_{scale}^2}, \quad N^2 = g\alpha\Delta T_v / D \quad (2.6 \text{ a,b})$$

It is presumed that

$$E_h \ll 1, \quad E_v \ll 1,$$

$$S \ll 1. \quad (2.7 \text{ a,b,c,d})$$

$$\sigma_v, \sigma_h = O(1)$$

so that the horizontal velocities are geostrophic to lowest order in regions, such as the interior of the basin, where the length scales chosen are appropriate to the motion. The limit of $S \ll 1$ implies that the scale of the basin, while small enough to neglect the beta effect is large with respect to the deformation radius.

For small Ekman numbers the velocity boundary conditions on the horizontal surfaces at $z = 0$ and d are the Ekman compatibility conditions, i.e.

$$w = \begin{cases} \frac{E_v^{1/2}}{2} \zeta(x, y, 0), & z = 0, \\ -\frac{E_v^{1/2}}{2} \zeta(x, y, d), & z = d. \end{cases} \quad (2.8 \text{ a,b,c})$$

$$\zeta = \left(\frac{\partial v}{\partial x} - \frac{\partial u}{\partial y} \right)$$

Since $S \ll 1$ the vertical velocity in the interior is $O\left(\frac{E_h}{S}, \frac{E_v}{S}\right)$ which is much larger, by $O(S)$ than the vertical derivative of w which is $O(E_h, E_v)$ from the vertical vorticity equation. This means that to lowest order the vertical velocity in the interior is independent of z and using geostrophy and the hydrostatic balance, both valid in the interior, it is easy to show (Pedlosky et. al. 1997) that for the interior,

$$w = w_I(x, y) = -\frac{E_v^{1/2}}{4} \nabla_h^2 \int_0^d T dz \quad (2.9)$$

so that the temperature equation for the interior reduces to:

$$R \frac{\partial \theta}{\partial z^2} + \nabla_h^2 \theta = 0,$$

$$\theta = T + \gamma R \int_0^d T dz, \quad (2.10, a,b,c,d)$$

$$\gamma = \frac{\sigma_v S}{2E_v^{1/2}}, \quad R = \frac{E_v \sigma_h}{E_h \sigma_v} = \frac{\kappa_v L_{scale}^2}{\kappa_h D^2}$$

Note that in terms of θ , the boundary conditions are the same as for T . Once θ is found, T is determined from:

$$T = \theta - \frac{\gamma R}{1 + \gamma R d} \int_0^d \theta dz, \quad (2.11)$$

while the pressure field, and hence the geostrophic velocities are determined from the hydrostatic relation, the thermal wind and the boundary condition (2.9) so it follows that

$$p = p_I = \int_0^z T_I dz' - \frac{1}{2} \int_0^d T dz \quad (2.12)$$

On the side walls there is a double boundary layer structure as discussed in Barcilon and Pedlosky (1967). There is an outer layer, the hydrostatic layer, whose non-dimensional width is

$$\delta_H = (\sigma_H S)^{1/2} \quad (2.13)$$

The velocity tangent to the boundary remains geostrophic in this layer and the vertical velocity is balanced by the horizontal diffusion of temperature while the vortex stretching in the layer is balanced by horizontal diffusion of vorticity. The motion remains in hydrostatic balance and thus the thermal wind relation holds for the shear of the tangent component of the velocity. We consider the total solution in this region to be a sum of the interior solution plus a boundary layer correction for each variable where the correction is denoted by an overbar. It follows from the above balances that the total vertical mass flux in the hydrostatic layer is, for example at $x=0$,

$$T_{rH} = (\sigma_h S)^{1/2} \int_0^\infty \bar{w}(\xi) d\xi = -\frac{E_h}{2\sigma_h S} \frac{\partial \bar{T}_o}{\partial \xi}(0) \quad (2.14)$$

where ξ is the stretched boundary layer variable, $\xi = x/\delta_H$. The temperature correction itself is scaled so that the temperature correction in the layer is $\delta_H \bar{T}_o$. On the other hand, since the tangential velocity parallel to the boundary satisfies the thermal wind relation,

$$\frac{\partial \bar{T}_o}{\partial \xi} = \frac{\partial \bar{v}_o}{\partial z} \quad (2.15)$$

In addition to the hydrostatic layer an even thinner buoyancy layer, whose width is

$$\delta_B = \frac{E_H^{1/2}}{(\sigma_H S)^{1/4}} \left(\frac{D}{L_{scale}} \right)^{1/2}. \quad (2.16)$$

in which, again, the vertical velocity is balanced in the heat equation by lateral diffusion of temperature. Hence its vertical transport of mass is related to its contribution to the temperature in a manner similar to (2.14). If a circumflex denotes an additional contribution to each field by the buoyancy layer, it follows that the total vertical mass flux in the buoyancy layer on each wall, for example at $x=0$, is,

$$T_{rB} = -\frac{E_H}{2\sigma_H S} \frac{\partial \hat{T}}{\partial \eta}(0) \quad (2.17 \text{ a,b})$$

$$\eta = x/\delta_B$$

The motion is no longer hydrostatic in this layer and the thermal wind equation no longer applies. The reader is referred to Barcilon and Pedlosky (1967) and Pedlosky et. al. (1997) for details.

We need not discuss the dynamics of the hydrostatic layer or buoyancy layer in detail only the following facts, easily demonstrated from the above references suffice.

The tangential velocity contribution by the buoyancy layer is smaller than either the interior tangential velocity or the hydrostatic layer's contribution at, say, $x=0$. Thus at that wall,

$$v_I + \bar{v} = 0, \quad x = 0. \quad (2.18)$$

The vertical derivative of (2.18) plus the thermal wind relation implies that at $x=0$

$$\frac{\partial \bar{T}}{\partial \xi} + \frac{\partial T_I}{\partial x} = 0, \quad x = 0. \quad (2.19)$$

This implies that the interior plus hydrostatic layer variables automatically satisfy both the no slip condition on the tangential velocity *and* the insulating condition on the temperature without the need for the buoyancy layer on this wall. This is clearly also true on all three insulating walls. Note too, that once the interior temperature field has been determined from the solution of (2.10 a) both the interior mass flux and the hydrostatic

layer's mass flux is determined. The solution for θ , of course, will require that we specify a boundary condition for that problem which discussion we momentarily defer.

On the fourth side, at $x=L$, the situation is more complex although again we will avoid a detailed description of the boundary layer dynamics since only certain gross characteristics of the boundary layer dynamics are important for the argument. The size of the vertical velocity in the buoyancy layer is determined by the fact that the layer can not have a net transport of order greater than the sum of the interior and hydrostatic layers. This sets an upper limit on the size of the boundary layer correction of the buoyancy layer to the temperature field. It is easy to show this correction, compared to the interior temperature is $O(\delta_B)$ (note that here $\eta = (L-x)/\delta_B$) and hence negligible. The temperature correction of the hydrostatic layer is similarly of $O(\delta_H)$ (which is why its temperature gradient balances the interior's temperature gradient on the other boundaries). Thus on this wall the *interior* temperature must satisfy the condition $T=0$ or equivalently, $\theta=0$ on $x=L$. Once again the hydrostatic layer is used to satisfy the no slip boundary condition on the velocity tangent to the wall. The thermal wind equation implies again, that the normal derivative of the sum of the interior temperature and the hydrostatic layer's temperature vanish at the wall. Thus on all four boundaries we have:

$$\nabla T_I \cdot \hat{n} + \nabla \bar{T} \cdot \hat{n} = 0 \quad (2.20)$$

where \hat{n} is the outward normal unit vector at the boundary. Note that this arises as a consequence of the geostrophy of the tangent component of velocity and the hydrostatic relation and not the thermal condition. It follows that on three of the four sides of the basin the thermal condition is automatically satisfied by the interior and hydrostatic layers but not on the fourth side where the fluid is free to exchange heat with its surroundings and satisfies the condition $T=0$, a condition we have seen must be satisfied by the interior temperature field. Hence it follows from (2.10b) that θ must vanish at $x=L$ i.e.

$$\theta = 0, \quad x = L \quad (2.21)$$

On the other hand the geostrophic velocity normal to the wall must vanish and the dominant contribution to the normal velocity comes only from the interior fields (the boundary layer portions contribute corrections to the normal velocity only of order of the boundary layer thickness). The vertical derivative of that condition plus the thermal wind balance implies that T and hence θ must be independent of distance along the boundary since the interior velocity is geostrophic. It follows from (2.21) that $\theta = 0$ on all the lateral boundaries which completes the specification of the interior problem.

Before examining a particular example note that the total interior vertical transport using (2.4e) and the divergence theorem, satisfies:

$$\int_0^l \int_0^L w_I dx dy = \frac{E_H}{2\sigma_h S} \oint_C \nabla T_I \cdot \hat{n} dl + \int_0^l \int_0^L \frac{\partial^2 T_I}{\partial z^2} dx dy \quad (2.22)$$

where C is the bounding contour of the basin. On the other hand, using (2.14) the total mass flux in the hydrostatic layer on all four lateral boundaries is:

$$T_{rH} = \frac{E_H}{\sigma_h S} \oint_C \nabla \bar{T} \cdot \hat{n} dl \quad (2.23)$$

hence, when (2.20) is used the sum of the interior vertical transport and the transport in the hydrostatic layers is:

$$T_{rI} + T_{rH} = \frac{E_v}{2\sigma_v S} \int_0^L dx \int_0^l dy \frac{\partial^2 T_I}{\partial z^2} \quad (2.24)$$

This total mass flux must be balanced by the vertical mass flux in the buoyancy layer as given by (2.17). Integrating over the single edge of the basin at $x=L$ where the buoyancy layer is active then yields:

$$\frac{E_v}{2\sigma_v S} \int_0^L dx \int_0^l dy \frac{\partial^2 T_I}{\partial z^2} - \frac{E_h}{2\sigma_h S} \int_0^l \frac{\partial \hat{T}}{\partial \eta}(0) dy = 0 \quad (2.25)$$

This condition turns out to be sufficient to determine the average value in y of all variables in the buoyancy layer although we do not need the solution for the purposes of this study. If (2.25) is integrated in the vertical from $z=0$ to $z=d$ and the boundary condition on the interior temperature at the upper surface, (2.3d) is used we obtain the heat balance for the basin as a whole, namely,

$$\int_0^l \int_0^L h dx dy - \frac{1}{R} \int_0^l \int_0^l \frac{\partial \hat{T}}{\partial \eta} dy dz = 0, \quad (2.26)$$

which states that the heat put into the basin at the upper surface is removed by conduction through the non insulated side wall by the temperature flux of the buoyancy layer. Note that on this boundary η and x derivatives have opposite signs since $\eta = (L - x)/\delta_B$ and so a positive h (heat flux into the basin) corresponds to a negative x -derivative of the buoyancy layer temperature (on average) on the fourth wall indicating heat flow out of the basin. If h were negative (cooling) all signs would simply be reversed for this linear problem.

Thus, the condition that the mass flux be balanced in the basin automatically satisfies the total heat balance. One might also imagine replacing the diffusive heat exchange through the fourth wall by an advective exchange were it truly an open boundary. In that case since (2.25) prescribes the heat exchange at each level z , and the temperature of the fluid is set to

match the temperature of the larger ocean to which it is connected, the mass flux could be determined.

The principal concern goal of this study is the ratio T_{rH}/T_{rI} i.e. the ratio of the boundary layer vertical transport to the transport in the interior. For that purpose a simple example is illuminating.

3. An example

Consider the example in which the applied heating has the form:

$$h = h_{nm} \sin(n\pi x/L) \sin(m\pi y/l) \quad (3.1)$$

Obviously, a general heating distribution can be synthesized from a Fourier sum of such heating terms.

The solution of (2.10a) subject to the conditions that θ vanish on the lateral boundaries, that the vertical derivative satisfy (2.3 d, e) is:

$$\theta = h_{nm} \sin(n\pi x/L) \sin(m\pi y/l) \left[\frac{\cosh K_{nm} z}{K_{nm} \sinh K_{nm} d} \right] \quad (3.2 \text{ a,b})$$

$$K_{nm} = \frac{1}{R} \left\{ \left(\frac{n\pi}{L} \right)^2 + \left(\frac{m\pi}{l} \right)^2 \right\}^{1/2}$$

in terms of which the interior temperature, vertical velocity and pressure are, from (2.11) and (2.12):

$$T_I = h_{nm} \sin(n\pi x/L) \sin(m\pi y/l) \left[\frac{\cosh K_{nm} z}{K_{nm} \sinh K_{nm} d} - \frac{1}{K_{nm}^2} \left(\frac{\gamma R}{1 + \gamma R d} \right) \right] \quad (3.3)$$

and,

$$p_I = h_{nm} \sin(n\pi x/L) \sin(m\pi y/l) \frac{1}{K_{nm}^2} \left[\frac{\sinh K_{nm} z}{\sinh K_{nm} d} - \frac{\gamma R z + 1/2}{1 + \gamma R d} \right] \quad (3.4)$$

Note that for large values of γR ,

$$\gamma R = \frac{v_y}{\kappa_h} \frac{N^2}{f^2} \frac{D}{\delta_E}, \quad (3.5)$$

the vertical average of the interior temperature goes to zero as γR becomes large. The parameter γR effectively measures the ratio of the vertical velocity pumped out of the Ekman layer to that which is consistent with the interior stratification. When γR is large the interior is unable to absorb the vertical velocity from the Ekman layer and alters the interior flow so that the horizontal velocity satisfies the no-slip condition on its own with only a minor adjustment by the Ekman layers.

(3.4) implies that the pressure and hence the geostrophic velocity satisfies the relation:

$$p_I(x, y, 0) = -p_I(x, y, d) \quad (3.6)$$

For large values of the parameter γR the interior pressure field and geostrophic velocity will go to zero on the upper and lower boundaries of the fluid expunging the Ekman layers there to lowest order. At the same time the horizontal geostrophic velocity will flow along the isolines of the heating function $h(x, y)$ so that right below the surface the flow will be anti-cyclonic under heating and cyclonic under cooling. The vertical structure,

however is a strong function of the parameters. Figure 2 shows the profile of the pressure field, and hence the geostrophic horizontal velocity, for values of $\gamma R = 50$ and $\gamma R = 0.5$ for the case where $m=1, n=1$, i.e. a heating which is maximum in the middle of the basin and that vanishes on its boundaries. Note that for large γR the geostrophic velocity is almost everywhere cyclonic under heating except at the surface. This is in agreement with the experimental results of Pedlosky et. al. (1997).

The interior vertical velocity may be calculated either from (2.4e) or (2.9). We obtain,

$$w_I = \frac{E_v}{2\sigma_v S} \frac{\gamma R}{1 + \gamma R d} h_{nm} \sin(n\pi x / L) \sin(m\pi y / l) \quad (3.7 \text{ a,b})$$

$$= \frac{E_v}{2\sigma_v S} \frac{\gamma R}{1 + \gamma R d} h(x, y)$$

so that there is a simple, direct relation between interior heating (or cooling) and the vertical velocity in the interior. It is interesting to note that the result (3.7b) is general and follows directly from (2.4e) and the vertical integral of (2.9) in any geometry and lateral boundary condition. To calculate the total vertical mass flux in the interior it is useful to use (3.7a) for later comparison to the transport in the hydrostatic layer. We obtain for the total interior transport:

$$T_{rI} = \frac{E_v}{2\sigma_v S} \frac{\gamma R}{1 + \gamma R d} h_{nm} \frac{Ll}{nm\pi^2} \left[1 - (-1)^n \right] \left[1 - (-1)^m \right] \quad (3.8)$$

On the other hand using (2.20) and (2.23) we can easily obtain the total transport in the hydrostatic layers around the basin, i.e.

$$T_{rH} = \frac{E_v}{2\sigma_v S} h_{nm} \frac{Ll}{nm\pi^2} \left[1 - (-1)^n \right] \left[1 - (-1)^m \right] \left\{ \frac{K_{nm} \cosh K_{nm} z}{\sinh K_{nm} d} - \frac{\gamma R}{1 + \gamma R d} \right\} \quad (3.9)$$

their ratio is:

$$\frac{T_{rH}}{T_{rI}} = \left(\frac{1 + \gamma R d}{\gamma R} \right) \frac{K_{nm} \cosh(K_{nm} z)}{\sinh K_{nm} d} - 1 \quad (3.10)$$

Figure 3 shows the value of the ratio near the upper boundary i.e. near $z = d$. We see that for all values of γ most of the transport under the surface takes place in the side wall boundary layers, increasingly so for smaller values of R or equivalently of the product γR . We see from (3.5) that this enhancement is favored by strong horizontal temperature diffusion, which we may think of as an analogue of strong lateral eddy mixing of heat. For a laboratory system for which R is unity a ratio greater than one is favored by large values of $K_{nm} d$, i.e. a basin rather narrow in at least one direction. Figure 4 shows the profile of w integrated in y across the basin right below the surface of the fluid. The heating is of the form $\sin(\pi x / L) \sin(\pi y / l)$ and is positive. The interior vertical velocity is upward as expected but the upward vertical velocity across the basin is dominated by the motion in the hydrostatic layers at $x = 0$ and $x = L$. At the latter boundary the compensating mass flux in the very thin buoyancy layer is evident.

At deeper levels the vertical mass flux in the hydrostatic layer changes sign and, together with the buoyancy layer produces a compensating downwelling to balance the interior. That is, there is a reversal at depth of the boundary vertical velocity. Figure 5 shows the profile in z of the transport in the hydrostatic layer near $x = 0$ for $\gamma = 50$ and $R = 0.5$. There is a reversal of the direction of the transport at z approximately equal to 0.7 below which the transport in the hydrostatic layer helps balance the interior. This is not found in the nonlinear model of Spall (2002) and is a consequence of the weaker vertical penetration of the thermal signal in the linear model. Nevertheless, directly below the heating the boundary layer transport is, as figure 4 has shown, in the same direction and larger than the

interior vertical transport so that most of the directly forced vertical motion at shallow depths takes place near the boundary.

If we were to consider a laboratory situation in which the basin were circular and the heating *axially symmetric* with uniform boundary conditions corresponding to $T=0$ on the outer wall, we would have axial symmetry in all the fields in the interior and boundary layers. In that case the vertical mass flux in the interior and the hydrostatic layers would be balanced by the mass flux in the narrower buoyancy layer distributed symmetrically around the cylindrical basin. For example, if the heating function $h(r)$ where r_o is the basin radius, were of the form:

$$h = h_n J_o(\alpha_n r / r_o) \quad (3.11)$$

where J_o is the zero order Bessel function and α_n is the n^{th} zero of the Bessel function of order zero, it is easy to show that the ratio shown in (3.10) becomes:

$$\frac{T_{rH}}{T_{rI}} = \left(\frac{1 + \gamma R d}{\gamma R} \right) \frac{(\alpha_n / r_o) \cosh(\alpha_n z / r_o) - 1}{\sinh \alpha_n d / r_o} - 1 \quad (3.12)$$

clearly the same parametric dependence. For the laboratory one would take $R=1$ but Figure 3 still applies for the ratio.

3. Discussion

In the simple model we have described here the mild heating (cooling) of the surface of a rotating stratified fluid leads to upwelling (downwelling) beneath the thermal forcing in the interior of the fluid. However the vertical velocities are small there since the rate at which fluid can rise or sink is limited by its ability to expunge the temperature anomaly obtained by moving in the background field of stratification. At the same time the fluid must diffuse

away the vorticity produced by vortex tube stretching. Both yield a small value of vertical velocity. In the boundary layer on the basin's lateral boundary motion on the scale of the deformation radius is able to more easily overcome these constraints through enhanced vorticity diffusion through the boundary or thermal diffusion into the interior. As a result in the simple example described in the preceding section the ratio of boundary layer to interior vertical transport in the upper region of the fluid directly under the thermal forcing is many times greater than unity. This apparently non-intuitive result is in qualitative agreement with the calculations of Spall (2002). It is interesting to note that Spall used both a complete primitive equation model (the MIT model, Marshall et. al. 1997) and a simple parameterization of eddy mixing which however, is substantially different than the linear model described here. The agreement of the analytical theory described here and the model results of Spall suggest that this partition of the vertical transport in favor of the side wall boundary layer is a general result and, as Spall, suggests, is connected to the need for the fluid to deal with both the buoyancy and vorticity anomalies which arise from strong vertical motion rather than a feature specific to any particular eddy dynamics. It would be of great interest to examine the question in a laboratory setting in which the heating can be controlled to examine the dependence of this ratio as the degree of nonlinearity in the motion field increases. Clearly, the neglect of nonlinearity is one of the weaknesses of the present study and it will be of interest to extend the present results into the nonlinear domain.

Acknowledgement : This research was supported in part by the National Science Foundation OCE- 9901654.

References

- Barcilon, V. and J. Pedlosky, 1967. Unified linear theory of homogeneous and stratified rotating fluids. *J. Fluid Mechanics*. **29**, 609-621
- Marshall, J.C., C. Hill, L. Perelman, and A. Adcroft. 1997. Hydrostatic, quasi-hydrostatic and non-hydrostatic ocean modeling. *J. Geophys. Res.* **102**, 5733-5752.
- Pedlosky, J. 1977. On coastal jets and upwelling in bounded basins. *J. Phys. Ocean.* , **4**, 3-18.
- Pedlosky, J., J.A. Whitehead, and G. Veitch, 1997. Thermally driven motions in a rotating stratified fluid, theory and experiment. *J. Fluid Mechanics*. **339**, 391-411
- Spall, M. A., 2002 On the thermocline circulation in semi-enclosed marginal seas. *J. Marine Res.* (submitted).

Figure Captions

Figure 1: The rectangular basin containing the fluid. The dimensions shown are non dimensional. See the text for the scales used.

Figure 2. The vertical profile of pressure (and thus the interior geostrophic velocity) for the example described in the text for $R=0.1$, $L=1$, $l=1$, $d=1$, and a) $\gamma=500$ and b) $\gamma=5$.

Figure 3. The ratio of the boundary layer vertical transport to the interior vertical transport near the upper surface of the fluid as a function of γ for three values of R . (0.5, 1, 2).

Figure 4 The profile of the vertical velocity, integrated in y across the basin as a function of x when $h = h_{11} \sin(\pi x/L) \sin(\pi y/l)$. Note that the vertical velocity in the interior is very small compared to the boundary layer contribution. In the case shown the h is positive and the non-dimensional velocity is scaled with $(E_v / \sigma_v S) / h_{11}$. The profile is given at $z=.99d$, $L=1$, $l=1$, and $\gamma=50$ while $R=0.5$. Note that the area under region of positive w does not balance the downwelling since the upward transport in the boundary layers on $y=0$ and $y=l$ are not included.

Figure 5 a) The vertical transport in the hydrostatic layer near $x=0$ as a function of z for $\gamma=50$, $R=0.5$. Note the reversal of the direction of the transport at $z=0.7$. b) w as a function of x , as in figure 4 but at $z=0.4d$.

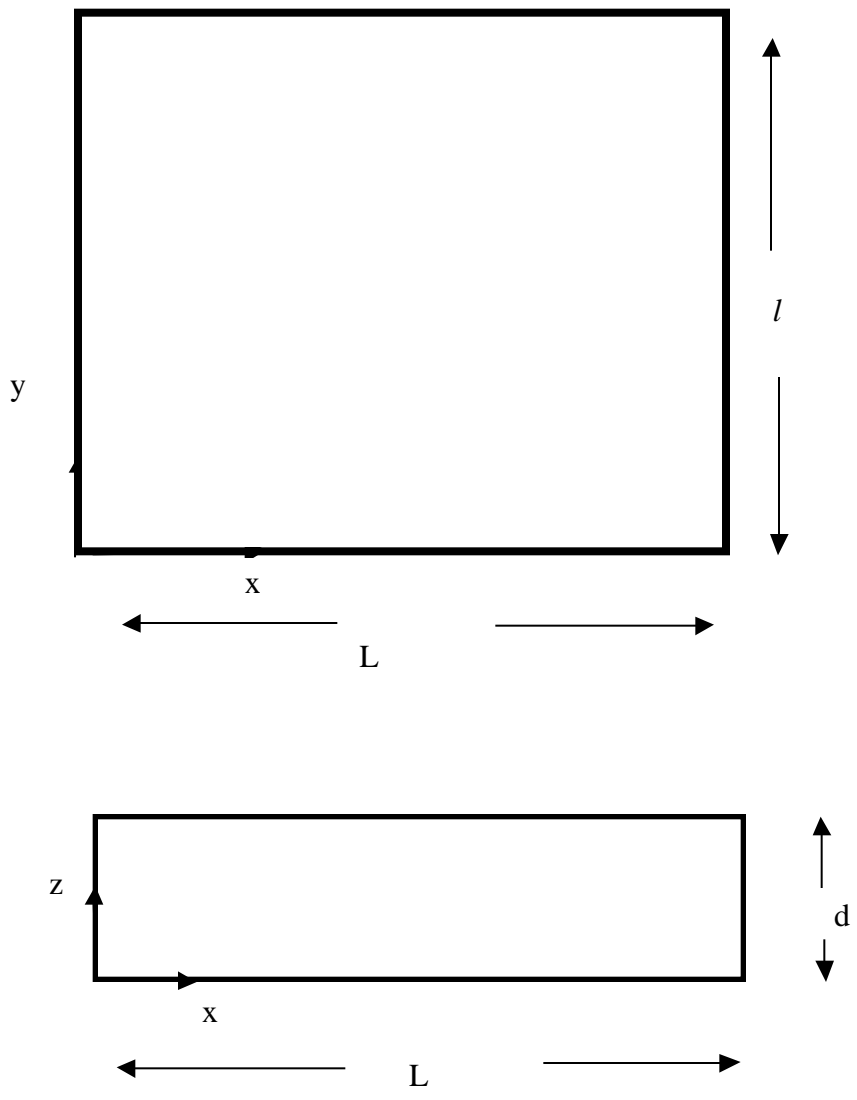


Figure 1

a)

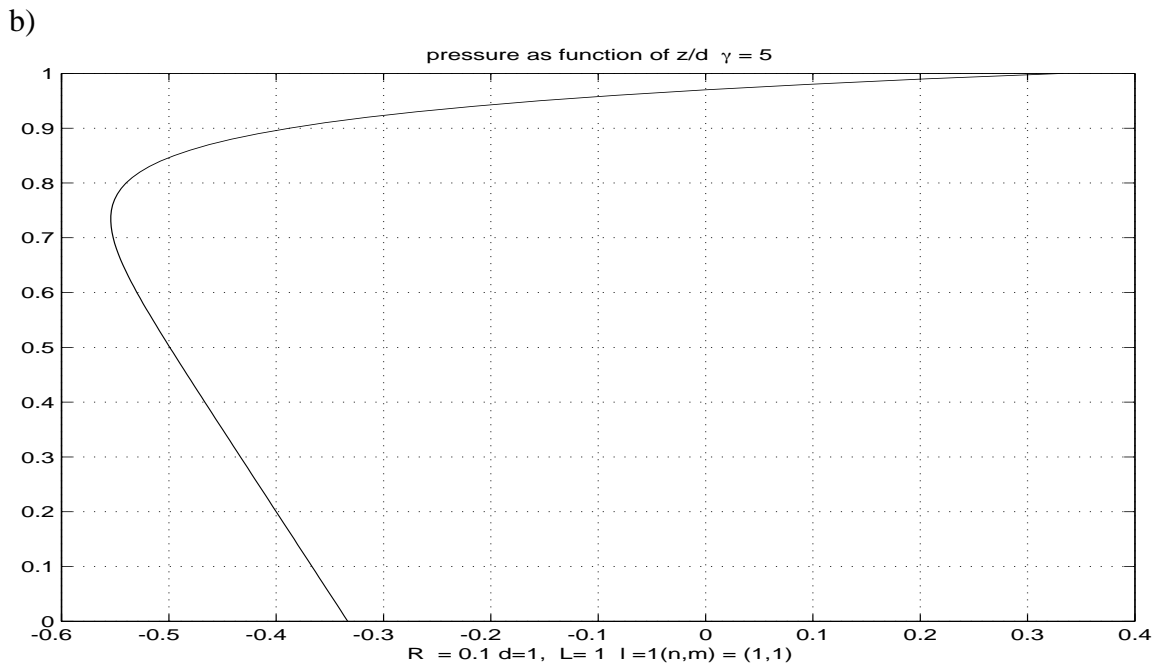
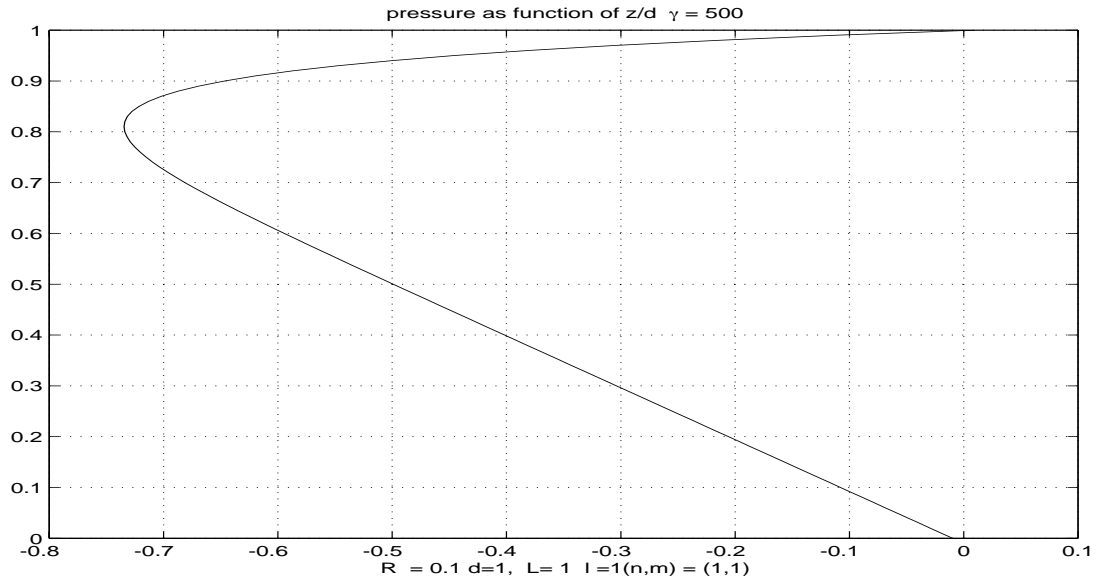


Figure 2

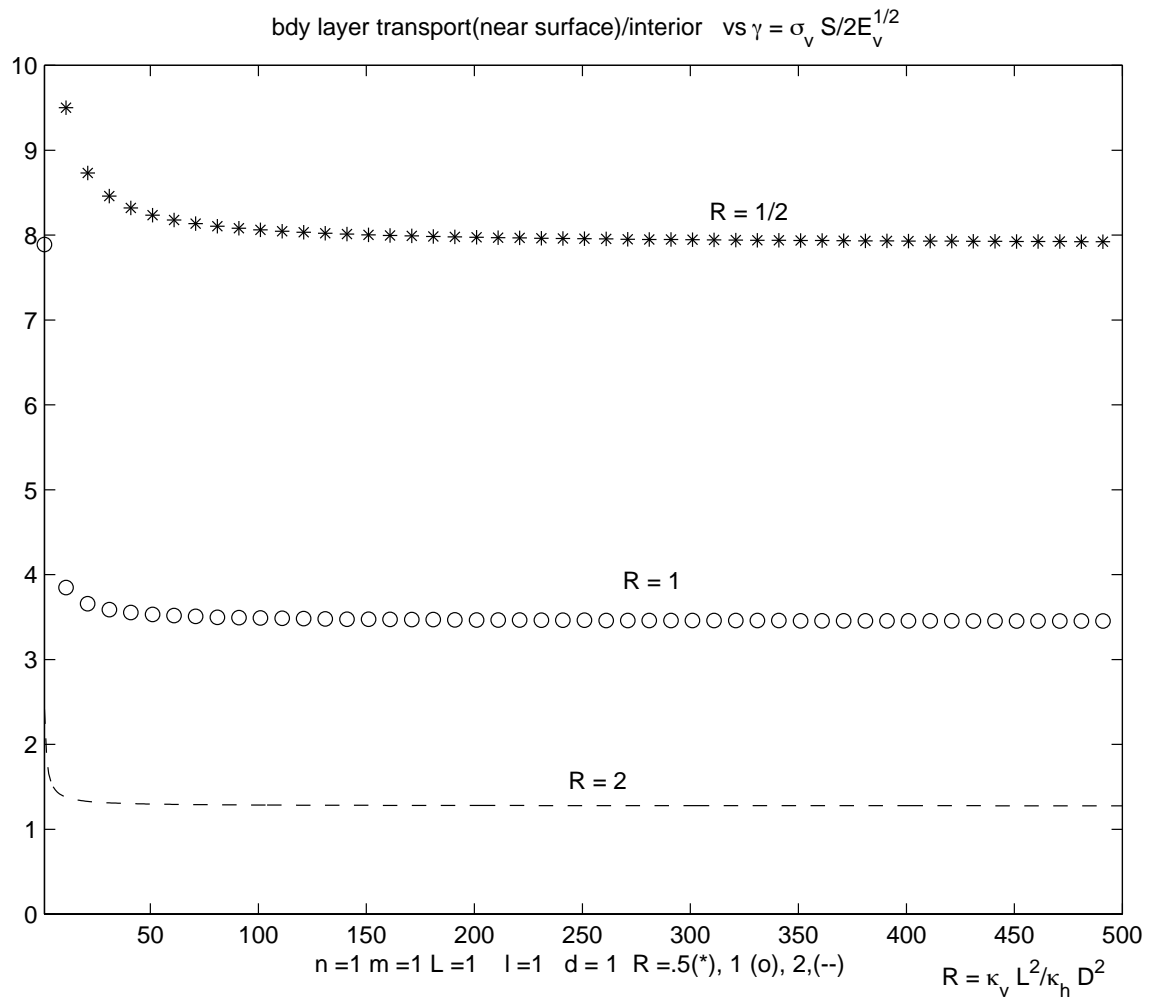


Figure 3

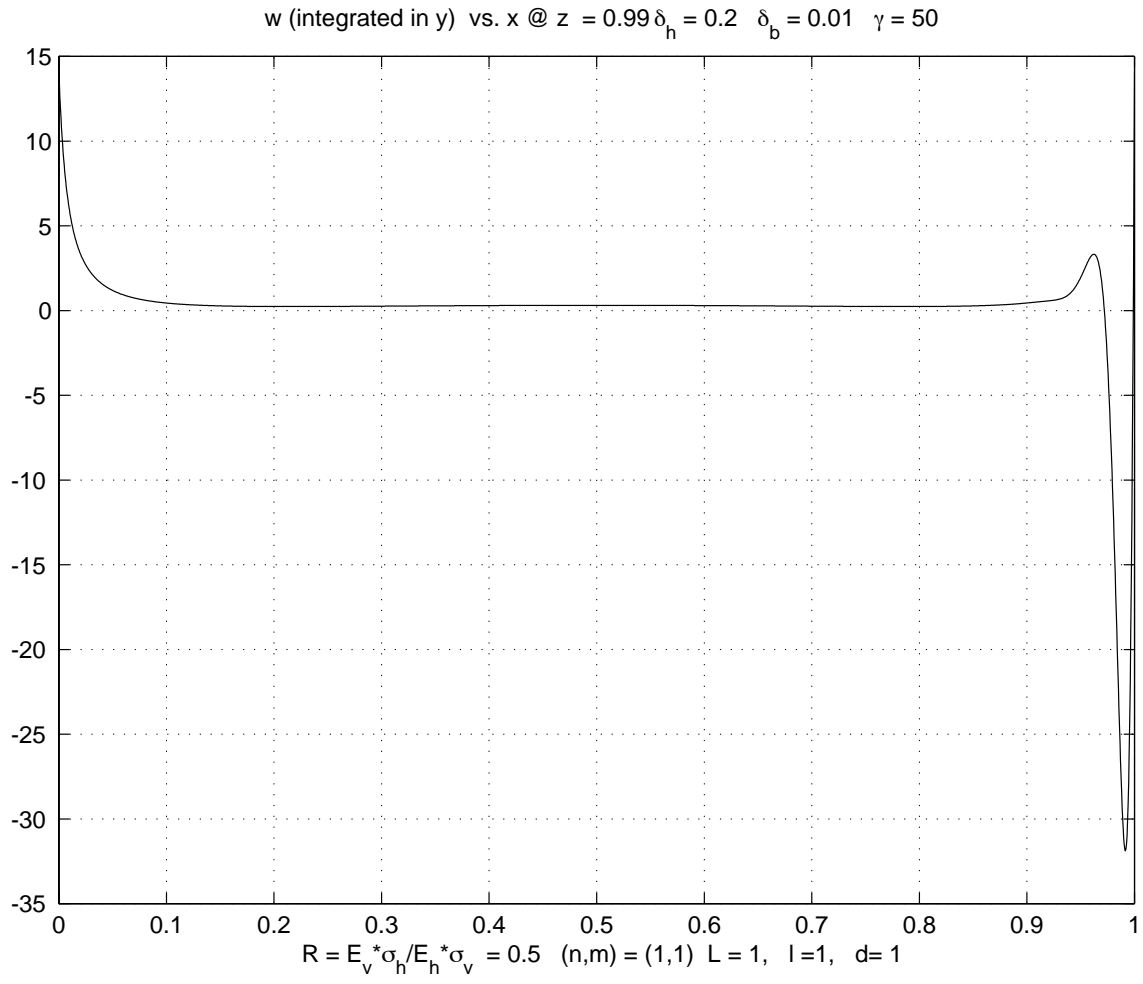
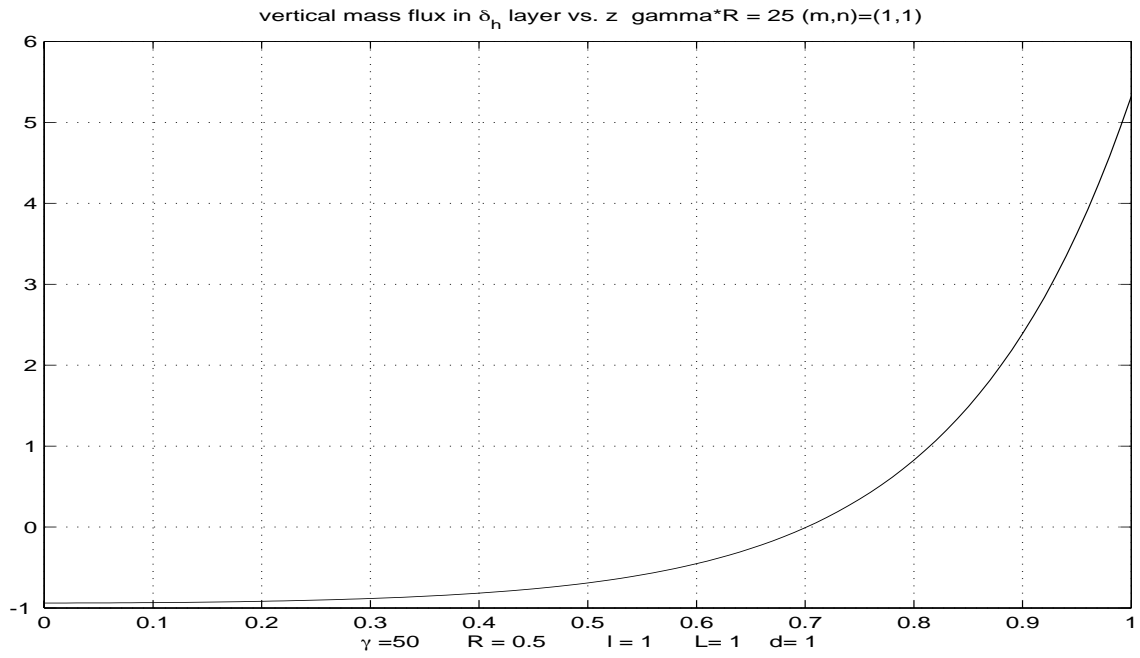


Figure 4

a)



b)

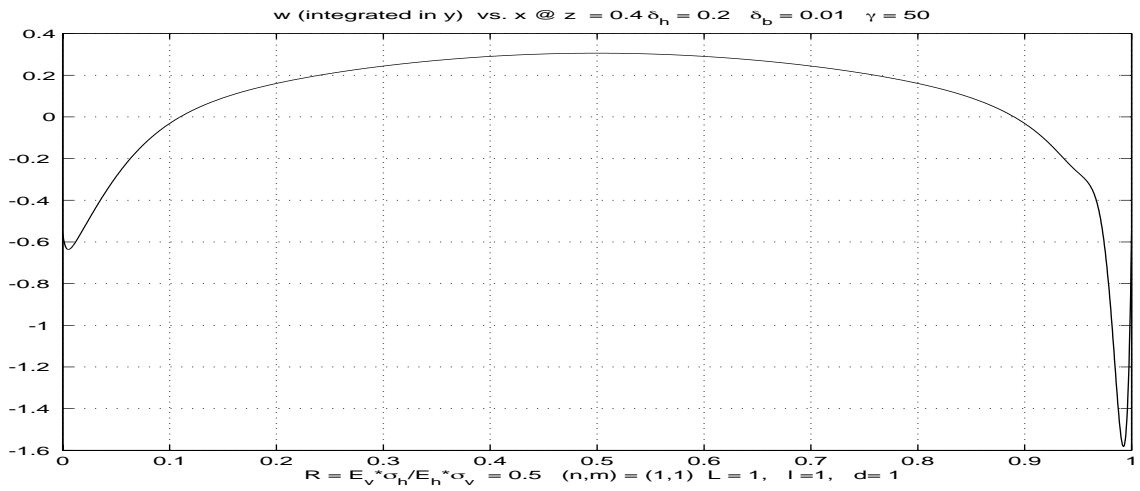


Figure 5